

Low-Temperature Photomagnetolectric and Photoconductive Effects in *n*-Type InAs[†]

S. S. Li and C. I. Huang

Department of Electrical Engineering, University of Florida, Gainesville, Florida 32601

(Received 19 April 1971)

A study of the photomagnetolectric (PME) and photoconductive (PC) effects in *n*-type InAs single crystals has been made between 4.2 and 300 °K under small-signal conditions. It was found that for $T > 77$ °K the PME open-circuit voltage is proportional to the magnetic induction, and for $T < 21$ °K the PME open-circuit voltage saturates at large magnetic induction, which is in accord with the large-Hall-angle PME theory. Carrier lifetimes were computed from the PME and PC data between 4.2 and 300 °K, and the hole mobility was estimated from the PME data at 21 and 4.2 °K. The observed linear relationship between the PME open-circuit voltage and photoconductance at low light levels manifests that the effect of trapping is essentially nil over the entire temperature range from 4.2 to 300 °K.

I. INTRODUCTION

The room-temperature photomagnetolectric (PME) effect in both *n*- and *p*-type InAs was reported previously by Dixon.¹ The results were interpreted in terms of the large-Hall-angle PME theory² for *p*-type samples and of the small-Hall-angle PME theory³ for *n*-type samples.

In the present work we extended the experimental study of the PME and PC effects in single-crystal *n*-type InAs from room temperatures down to 4.2 °K. Incorporating the two measurements with resistivity and Hall-effect experiments would allow us to determine the carrier lifetimes as well as electron and hole mobilities at low temperatures. The carrier lifetimes were computed from the PME and PC data, and the electron and hole mobilities were deduced from the Hall effect and the PME data between 4.2 and 300 °K.

II. EXPERIMENTAL

Undoped *n*-type InAs grown by the Czochralski method with electron concentration of 2.4×10^{16} cm⁻³ was used in the present work. The sample was cut into rectangular form by using a diamond saw. The dimensions of the sample, after being mechanically lapped by SiC powder and chemically etched by CP₄, were $1.3 \times 0.4 \times 0.04$ cm³. The sample was then mounted onto the cryotip of the AC-310 refrigeration system. The resistivity

and Hall-effect measurements were performed by using the standard dc method. The PME and PC measurements were performed by using the ac method, similar to that described in Ref. 1. The tungsten lamp light source was chopped at 400 cps, and the PME and PC signals picked up from the sample were passed through amplifiers and a wave analyzer. The system provides a gain of 10^5 , which would allow us to measure a relatively small signal.

III. RESULTS AND DISCUSSION

The resistivity and Hall effect were measured between 4.2 and 300 °K. The results showed that the electron concentration was nearly constant over the entire temperature range, and the Hall mobility (assuming equal to electron mobility) reached a peak value at 77 °K. The results are summarized in Table I.

The PME open-circuit voltage and the photoconductance, as functions of magnetic induction and light intensity, were measured between 300 and 4.2 °K. The results for $T > 77$ °K were in accord with the small-Hall-angle PME theory, and for $T < 21$ °K, the large-Hall-angle PME theory predicted the observed PME data. This will be discussed separately.

A. Results for 77 °K < T < 300 °K

In this temperature range, the small-signal PME

TABLE I. Transport and recombination parameters for *n*-type InAs.

T (°K)	ρ (Ω cm)	R_H (cm ³ /C)	$n_0 = \frac{1}{R_H e}$ (10^{16} cm ⁻³)	μ_n^a (10^4 cm ² /V sec)	$b(\mu_n/\mu_p)$	μ_p (cm ² /V sec)	τ (sec)
300	0.0114	263	2.38	2.3	100	230	3.7×10^{-8}
78	0.00583	310	2.02	7.37	100	737	1.8×10^{-7}
21	0.0063	310	2.02	4.93	15	3290	2.1×10^{-8}
4.2	0.01	310	2.02	3.10	5	6200	4.75×10^{-9}

^aAssuming $\gamma_H = 1$, $\mu_H = \mu_n$.

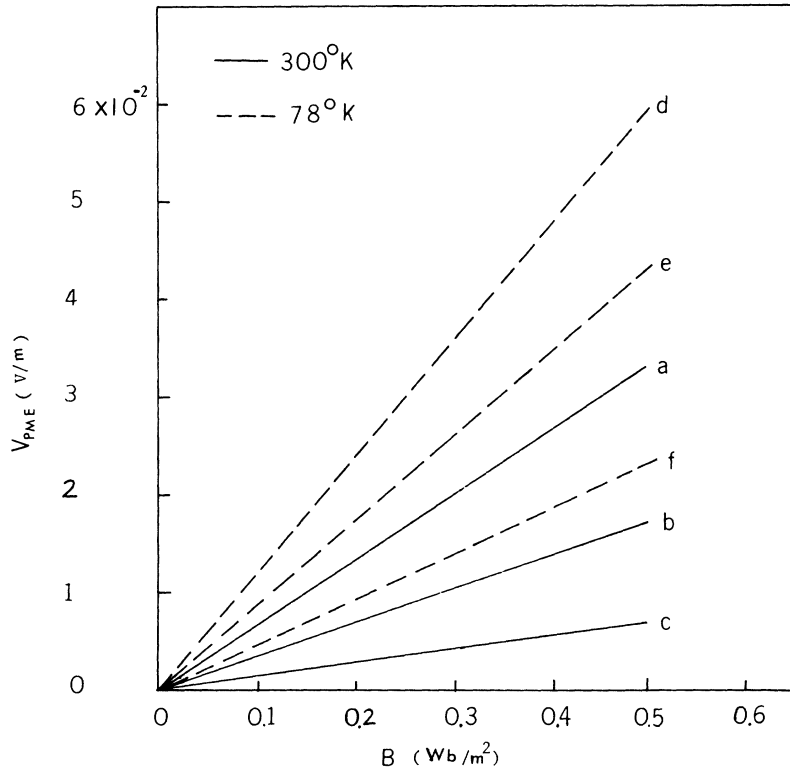


FIG. 1. PME open-circuit voltage per unit sample length, V_{PME} vs magnetic induction B with light intensity I_0 as a parameter for $T = 300$ and 77°K . Curves a $I_0 = 430 \text{ mW/cm}^2$, b 270 mW/cm^2 , c 81 mW/cm^2 , d 430 mW/cm^2 , e 224 mW/cm^2 , and f 129 mW/cm^2 .

and PC data are shown in Figs. 1 and 2. Figure 1 shows the PME open-circuit voltage V_{PME} vs the magnetic induction B for $T = 300$ and 77°K , with

light intensity I_0 as a parameter. The results are in accord with the small-Hall-angle PME theory given by Van Roosbroeck³ which leads

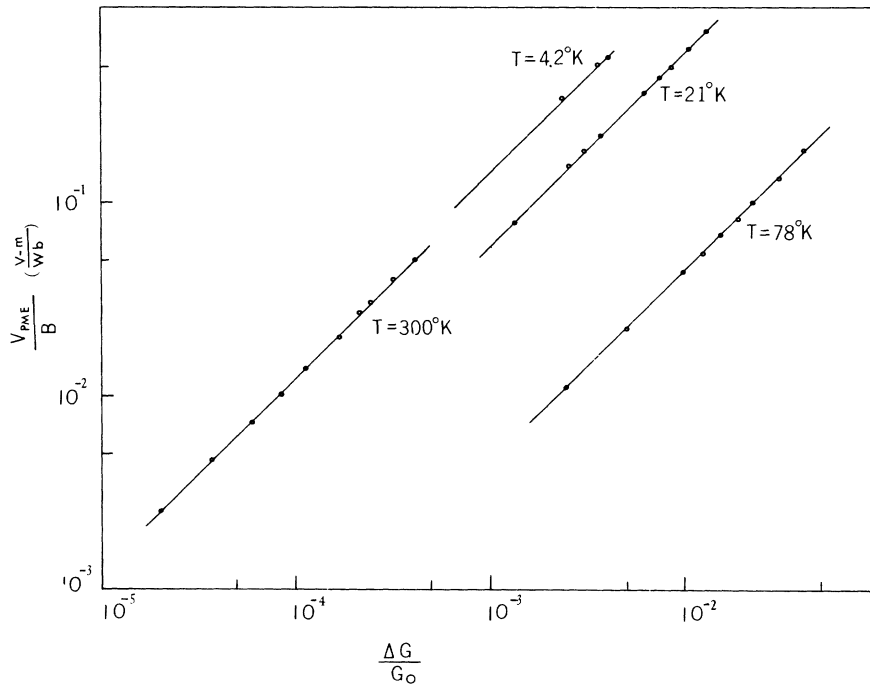


FIG. 2. PME open-circuit voltage V_{PME} vs photoconduc-tance ratio $\Delta G/G_0$ for $T = 300$, 77 , 21 , and 4.2°K . The slope of these plots is unity.

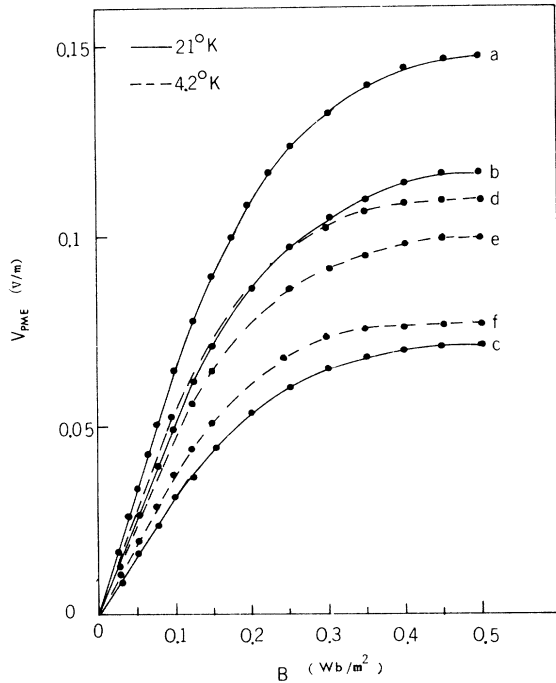


FIG. 3. PME open-circuit voltage per unit sample length V_{PME} vs magnetic induction B with light intensity I_0 as a parameter for $T = 21$ and 4.2°K . Curves a $I_0 = 430$ mW/cm 2 , b 224 mW/cm 2 , c 81 mW/cm 2 , d 350 mW/cm 2 , e 156 mW/cm 2 , and f 106 mW/cm 2 .

$$V_{\text{PME}} = (D_p/\tau_p)^{1/2} B(\Delta G/G_0), \quad (1)$$

where D_p is the hole diffusion coefficient, τ_p is the hole lifetime, G_0 is the dark conductance, and ΔG is the photoconductance. The linear relationship between V_{PME} and B , observed at 77 and 300°K , indicates that the hole mobility is low in this temperature range. Assuming that the electron mobility equals the Hall mobility, and electron-hole mobility ratio of 100 , the hole mobility was estimated at 300 and 77°K (see Table I). The hole lifetime (which is equal to electron lifetime for the present case) is deduced from Eq. (1) and the PME data shown in Fig. 2. The carrier lifetime estimated at 300°K ($\tau = 3.7 \times 10^{-8}$ sec) is in good agreement with that reported previously by Dixon.¹ The substantial increase in the photoconductance at 77°K (as compared with value at 300°K) is due to the fact that both the carrier mobility and the carrier lifetime are increased substantially at 77°K .

B. Results for $4.2^\circ\text{K} < T < 21^\circ\text{K}$

In this temperature range, the V_{PME} saturates at high magnetic field strength, indicating that the hole mobility is greatly increased at low temperatures. To interpret the observed V_{PME} -vs- B plot as shown in Fig. 3, the large-Hall-angle PME theory is

used. The theory predicts that⁴

$$V_{\text{PME}} = \left(\frac{D_p}{\tau_p}\right)^{1/2} \frac{B}{(1 + \mu^2 B^2)^{1/2}} \frac{\Delta G}{G_0}, \quad (2)$$

where $\mu = (\mu_n \mu_p)^{1/2}$ is the effective carrier mobility. Equation (2) predicts that the V_{PME} is proportional to B at low magnetic field and is independent of B at high magnetic field. The results shown in Fig. 3 for $T = 21$ and 4.2°K are in accord with the prediction given by Eq. (2). To estimate effective mobility μ and hole lifetime τ_p from Eq. (2) and Fig. 3, a plot of $(B/V_{\text{PME}})^2$ vs B^2 is shown in Fig. 4. The intercept of the straight lines shown in Fig. 4 with the ordinate yields the hole lifetime and the slope of these lines yields the effective carrier mobility. The computed values of μ and τ_p at 21 and 4.2°K from Fig. 4 are summarized in Table I. The electron mobility is deduced from resistivity and Hall-effective measurements, and the hole mobility is computed from $\mu_p = \mu^2/\mu_n$. The results show that the electron and hole mobility ratio changes drastically from assumed value of¹ 100 at

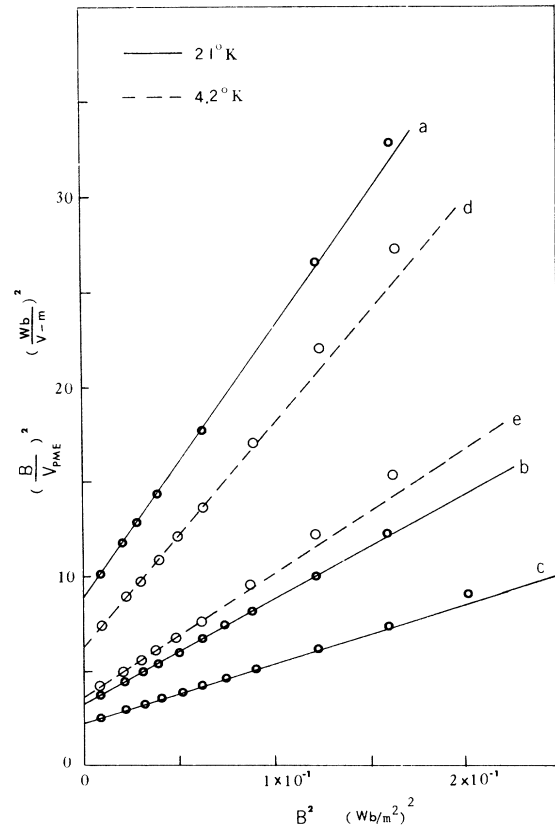


FIG. 4. $(B/V_{\text{PME}})^2$ vs B^2 with light intensity I_0 as a parameter for $T = 21$ and 4.2°K . The intercept of this plot with ordinate is equal to τ_p/D_p and the slope of this plot yields $(\tau_p/D_p)\mu^2$. Curves a $I_0 = 106$ mW/cm 2 , b 224 mW/cm 2 , c 430 mW/cm 2 , d 106 mW/cm 2 , and e 224 mW/cm 2 .

300 °K to the value of $b = 5$ (computed value) at 4.2 °K. This is indeed consistent with the observed $V_{\text{PME}}\text{-vs-}B$ data for T at 300 and 4.2 °K. The change in mobility ratio with temperature has also been observed in InSb.⁵

Figure 2 illustrates the plot of (V_{PME}/B) vs $\Delta G/G_0$ for $T = 300, 77, 21,$ and 4.2 °K. The results (slope of this plot is one) at all temperatures show that no trapping effect is involved in the entire temperature range.^{6,7} It is noted in Fig. 4 that the deviation from linearity [as is predicted by Eq. (5)] at higher magnetic field is due to the fact that the photoconductance becomes magnetic field dependent as B is increased.

[†]Research supported in part by the Advanced Research Projects Agency, and monitored by AFCRL under Contract No. F19628-68-C-0058.

¹J. R. Dixon, Phys. Rev. **107**, 374 (1957).

²S. W. Kurnick and R. N. Zitter, J. Appl. Phys. **27**, 278 (1956).

³W. van Roosbroeck, Phys. Rev. **101**, 1713 (1956).

⁴S. S. Li, Phys. Rev. **188**, 1246 (1969).

IV. CONCLUSIONS

Experimental study of the PME and PC effects in n -type InAs single crystals has been extended from room temperature down to 4.2 °K. The results are in good agreement with the theory developed previously. Carrier lifetimes and mobilities are deduced from the present results. Measurements of the PME and Hall effect at low temperatures enable us to determine both the majority and minority carrier mobilities in n -type InAs. Study of the PME and PC effects show that no trapping is involved in the entire temperature range for the present samples.

⁵R. N. Zitter, A. J. Strauss, and A. E. Attard, Phys. Rev. **115**, 266 (1959).

⁶S. S. Li and H. F. Tseng, Phys. Rev. B (to be published).

⁷There will be a nonlinear relationship between the V_{PME} vs G/G_0 plot in the presence of trapping of excess carriers [see, for example, J. Agraz and S. S. Li, Phys. Rev. B **2**, 1847 (1970)].

Phonon Dispersion in Noble Metals

P. K. Sharma and Narain Singh

Physics Department, University of Allahabad, Allahabad, India

(Received 10 May 1971)

The phonon dispersion relations in the three symmetry directions of the noble metals copper, silver, and gold at room temperature have been determined from a model for the lattice dynamics of metals recently propounded by Chéveau. The results agree reasonably well with recent neutron scattering experiments.

The lattice dynamics of metallic crystals has been the subject of investigation by many theoretical and experimental workers over the past several years.¹ In the last few years, a number of models²⁻⁵ have been developed for studying phonon dispersion in cubic metals, considering explicitly the presence of conduction electrons. Many of them, however, have not been able to stand the test of recent neutron scattering experiments. For example, the recent model of Krebs⁵ satisfies the symmetry requirements, but suffers from a serious lack of internal equilibrium and necessitates external forces to maintain the system in equilibrium. Quite recently Chéveau⁶ has propounded a model for the lattice dynamics of cubic metals which is free from these discrepancies. It satisfies the symmetry properties of a cubic lattice by using Lax's⁷ expression for the electron-ion interaction contribution and preserves internal equilibrium without recourse to external forces. The ion-

ion interaction is described by the first two terms in the Taylor expansion of the potential energy. This model has furnished a reasonably satisfactory description of the lattice vibrations in alkali metals,⁸ and of the temperature variations of the thermal expansion, Debye-Waller factors, and transport properties of a number of cubic metals.^{9,10} In this paper we report a study of phonon dispersion relations in noble metals on the Chéveau model. The motivation for this study was the recent appearance of detailed phonon dispersion curves for copper¹¹⁻¹³ and silver^{14,15} from experiments on coherent inelastic neutron scattering.

The secular equation determining the angular frequencies ω of the normal modes of vibration in a cubic metal can be written as

$$|M(\vec{q}) - m \omega^2 I| = 0, \quad (1)$$

where m is the mass of an atom in the lattice and